THE JOURNAL OF PHYSICAL CHEMISTRY B

Article

pubs.acs.org/JPCB

Dynamic Heterogeneity in the Monoclinic Phase of CCl_4

Nirvana B. Caballero,*[,†,‡] Mariano Zuriaga,*[,†,‡] Marcelo Carignano,*[,§] and Pablo Serra*[,†,‡]

[†]Facultad de Matemática, Astronomía y Física, Universidad Nacional de Córdoba, X5016LAE Córdoba, Argentina

[‡]IFEG-CONICET, Ciudad Universitaria, X5016LAE Córdoba, Argentina

[§]Qatar Environment and Energy Research Institute, Hamad Bin Khalifa University, P.O. Box 5825, Doha, Qatar

Supporting Information

ABSTRACT: Carbon tetrachloride (CCl_4) is one of the simplest compounds having a translationally stable monoclinic phase while exhibiting a rich rotational dynamics below 226 K. Recent nuclear quadrupolar resonance experiments revealed that the dynamics of CCl_4 is similar to that of the other members of the isostructural series CBr_nCl_{4-n}, suggesting that the universal relaxation features of canonical glasses such as α and β relaxation are also present in nonglass formers. Using molecular dynamics simulations we studied the rotational dynamics in the monoclinic phase of CCl_4. The molecules undergo $C3$-type jump-like rotations around each one of the four C−Cl bonds. The rotational dynamics is very well described with a master equation using as the only input the rotational rates measured from the simulated trajectories. It is found that the heterogeneous dynamics emerges from faster and slower modes associated with different rotational axes, which have fixed orientations relative to the crystal and are distributed among the four nonequivalent molecules of the unit cell.

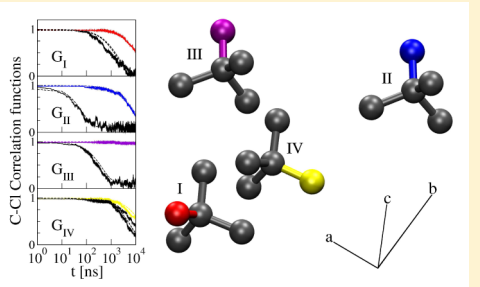

INTRODUCTION

The currently accepted scenario for canonical glasses includes different relaxation mechanisms that are universally present in all systems. Experimentally, these different mechanisms are clearly revealed by the dielectric spectra that show a broad low-frequency peak referred to as α-relaxation[1,2] and a higher frequency peak or shoulder usually called Johari−Goldstein β-relaxation.[3−14] The α-relaxation is generally attributed to processes involving the cooperative dynamics of regions of molecules.[1,2] The microscopical origin of the β relaxation is still a matter of wide debate.[4−13] The proposed models explain this peak as a consequence of the nonuniformity of the glassy state involving only local regions in which molecules can diffuse (islands of mobility). An alternative homogeneous explanation attributes the secondary relaxation phenomena to small-angle reorientations of all of the molecules.[15−17]

Systems having translational crystalline order but rotational degrees of freedom also display a glassy behavior. Because in these cases one type of degree of freedom is completely absent, they represent simplified models on which to test theoretical concepts on glassy dynamics.[18−21] Compounds of molecules of the type CBr_nCl_{4-n}, with n = 0,1,2, are examples of systems with this characteristics.[22−24] They have a series of solid−solid phase transitions attributed to the ability of the molecules to acquire rotational degrees of freedom as the temperature is increased. All of these compounds crystallize from the melting to a plastic FCC phase. Further reduction of the temperature leads to a $C2/c$ monoclinic phase.[25−29] The cases n = 1 and 2 exhibit a glass transition at 90 K that is clearly visible through calorimetric techniques, and its structure shows disorder in the position of the Cl and Br atoms.[30,31] The case n = 0 cannot display such a disorder, and, in fact, the calorimetric curve does not show a glass transition at low temperatures.[30]

The dielectric spectra of $CBrCl_3$ and CBr_2Cl_2 were reported by Zuriaga et al.[24] in the temperature range 100−250 and 100−210 K, respectively. At the lower end of the temperature range the most relevant characteristic is that both spectra display a well-defined shoulder on the high frequencies flank of the α-peak, which is attributed to the β-relaxation. Because CCl_4 has no molecular dipole moment it is not accessible to dielectric experiments, but it can be studied using nuclear quadrupolar resonance. Interestingly, the resolution of the NQR spectra for CCl_4 is well superior to the corresponding spectra for CBr_2Cl_2 and $CBrCl_3$ and the two techniques complement each other. On the contrary, the NQR experiments are limited to a temperature range between 77 and 140 K, with the upper end determined by the broadening of the signal. The picture that emerges from the combined analysis is that the three compounds have a very similar dynamic evolution in the monoclinic phase as a function of temperature.[23,24] The analysis of the isostructural CCl_4 shows that nonequivalent molecules in the unit cell perform reorientational jumps on different time scales due to their different crystalline environments. These results support the conclusion that the dynamic heterogeneity is intimately related to the secondary relaxation observed in these compounds.[23,24,32]

This work is a direct extension of our previous works involving halogenomethanes.[23,24,32] In this case we have studied

Received: November 29, 2015
Revised: January 11, 2016

DOI: 10.1021/acs.jpcb.5b11658
J. Phys. Chem. B XXXX, XXX, XXX−XXX

the monoclinic phase of CCl_4 using extensive molecular dynamics simulations on a fully anisotropic cell, and the results were compared with an analytical stochastic model. The advantage of this particular system is that it allows for the determination of rotational correlation times from NQR measurements with sufficient precision to distinguish between the nonequivalent groups of molecules. The same distinction is easily done in the molecular dynamics simulations, which, in turn, allows for an analysis at the individual nonequivalent groups and correlates the results with the location of the molecules in the lattice. The temperature range affordable by the simulations covers from the FCC phase down to 160 K. Simulations at lower temperatures became impossible as the relaxation times go beyond 10 μs. It is found that when the spin−lattice relaxation times from the experiments and from the simulations are plotted in the 100−220 K temperature range the two sets of curves correspond to each other very well for the five distinguishable modes, suggesting that CCl_4 behaves as a strong glass in the whole temperature range, despite the fact that the compound cannot glassify due to its lack of orientational entropy.

THEORETICAL METHODS

Model and Computational Details. CCl_4 is a tetrahedral molecule having three equivalent C_2 and four equivalent C_3 symmetry axes. Following our previous work,[32] we have modeled the CCl_4 molecule as a rigid, nonpolarizable tetrahedron with the carbon atom at its center and a chlorine atom at each one of the vertices. The interaction between molecules is represented by a combination of Lennard-Jones and Coulombic terms summarized in Table 1. The cross

Table 1. CCl_4 Model Parameters and Geometry

	ϵ (kJ/mol)	σ (nm)	q (e)	bond (nm)	
C	0.22761	0.37739	−0.696	C−Cl	0.1766
Cl	1.09453	0.34667	0.174	Cl−Cl	0.2884

interaction between atoms of different type is calculated by applying the Lorentz−Berthelot combination rules, that is, geometrical mean for ϵ and arithmetic mean for σ. A spherical cutoff at 1.5 nm was imposed on all intermolecular interactions. Periodic boundary conditions were imposed in all three Cartesian directions.

The monoclinic crystal structure of CCl_4, resolved by Cohen et al. at 195 K,[33] corresponds to the $C2/c$ space group. The unit cell, which contains $Z = 32$ molecules, has the following lattice parameters: $a = 2.0181$ nm, $b = 1.1350$ nm, $c = 1.9761$ nm, and angle $\beta = 111.46°$. Using the experimental crystalline structure as initial coordinates, we constructed a simulation supercell containing 512 molecules, which correspond to 16 monoclinic unit cells. This supercell was prepared by replicating the experimental unit cell twice on the x and z directions and four times in the y direction.

The molecular dynamics simulations, conducted under NPT conditions, have been carried out using the Gromacs v5.0.2 simulation package. Atom−atom distances within each molecule were kept constants with the SHAKE algorithm. The simulations were started with a 10 ns equilibration run with the pressure controlled by a Berendsen barostat and the temperature controlled with the v-rescale thermostat. The Berendsen weak coupling method ensured a smooth approach to equilibrium with no disruptions to the simulation cell. The classical Newton's equations were integrated using the leapfrog algorithm, and the time step of the integration of the equations of motion was set to 1 fs.

The production runs were extended up to 100 ns or 10 μs depending on the temperature, using in this case a time step of 5 fs. The control of the temperature was made by using a Nosé−Hoover thermostat with a time constant of 2.0 ps. The pressure was maintained constant by using a fully anisotropic Parrinello−Rahman barostat with a reference pressure of 1 atm. The study covered temperatures ranging from 160 to 230 K in steps of 10 K. The monoclinic structure was stable in the whole analyzed temperature range (see Supporting Information).

RESULTS AND DISCUSSION

The spatial positions of the molecules in the unit cell of the system are defined through the application of eight symmetry operations over the four nonequivalent molecules (16 Cl atoms with nonequivalent positions). As a consequence, the system has four distinctive groups of molecules that we will refer to as G_I, G_{II}, G_{III}, and G_{IV}. In our simulation cell, each group contains 128 molecules. Each molecule belonging to a given group has the same specific arrangement of neighboring molecules. All of the molecular reorientation processes occurring during the simulations are sudden large-angle jumps of the Cl atoms. The jumps were detected using a running test algorithm based on a signal-to-noise measure and adapted from the work of Carter and Cross.[34] In this method, the molecular jumps are detected by a spike in the test function, as explained in the Supporting Information. After analyzing the trajectories for all of the temperatures, the time t_i of every single jump was registered. The angle described by a C−Cl bond upon a jump was calculated using the average direction of the bond before and after the jump. Namely, defining $\vec{b}_j$ as the bond between the central C atom and the jth Cl atom of the same molecule, the angle jump at time t_i is defined as the angle between $\langle \vec{b}_j \rangle_{i-1}$ and $\langle \vec{b}_j \rangle_i$. Here the angular brackets represent time average and the subscript i indicates the lapse between t_i and t_{i+1}. In Figure 1 we show the relative frequency of the reorientation angles calculated from the simulation at 160 K and for the four different groups of molecules. All of the curves peak at the

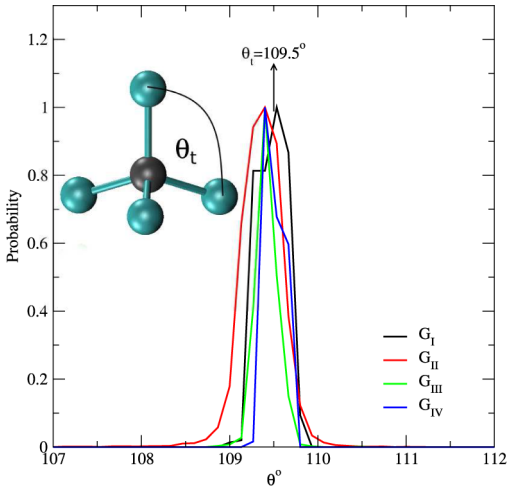

Figure 1. Normalized frequency distribution of reorientation angles for the four distinct group of molecules, as indicated. The results correspond to the production run at 160 K. The maximum at the tetrahedral angle indicates that all jumps are $C3$-type rotations.

DOI: 10.1021/acs.jpcb.5b11658
J. Phys. Chem. B XXXX, XXX, XXX−XXX

tetrahedral angle, which is the angle that should be observed upon C3-type rotations. Indeed, a careful inspection confirmed that for all temperatures there were just a handful of cases corresponding to C2-type rotations and therefore these were neglected in the analysis.

To characterize the molecular rotations using standard self-correlation methods, we calculate the relaxation of the bond orientation through self-correlation functions defined as

$$C_j(t) = \langle \vec{b}_j(0)\cdot\vec{b}_j(t)\rangle \quad (1)$$

where j = 1,...,4 represents a particular C−Cl bond, $\vec{b}_j(0)$ represents the position of the C−Cl$_j$ bond under the initial condition, and the angular brackets represent the average over the 128 molecules of the same group.

The resulting self-correlation functions are shown in Figure 2 with solid lines. Not only do the correlation times for the reorientations of the molecules depend on the groups but also the curves reveal that one bond (green lines) maintains its orientation for a time considerably longer than the other three bonds. This indicates that the molecules have preferential axes of rotation. G_{III} exhibit the strongest rotational anisotropy, followed by G_{II} and G_I, and only a minor effect is observed in G_{IV}. The strength of this anisotropic character decreases with increasing temperature as all of the free-energy barriers become relatively smaller.

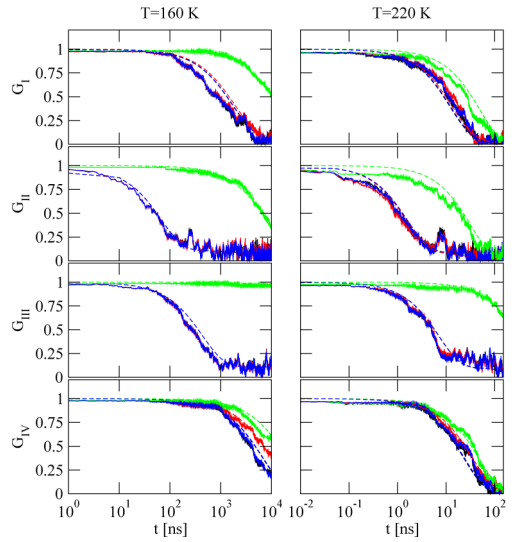

Figure 2. Autocorrelation functions $C_j(t)$ of the four bonds C−Cl$_j$ averaged over molecules within the four groups of the system. The solid lines correspond to the MD simulation results and the dashed lines are derived from the master eq 2. Different colors correspond to the four different bonds.

During a rotation of the type C3 one of the C−Cl bonds remains in its place and therefore one Cl atom does not change its average position. The remaining three Cl atoms undergo a jump of 109.5°. Each molecule has four possible axis for a C3 type rotation that coincide with the C−Cl molecular bonds. As all of the molecular bonds remain lying around the four initial orientations in the crystal it is possible to define, for each molecule, four axes of rotation relative to the overall orientation of the crystal. In this way we define the axes a_i, i = 1,...,4, for each one of the molecules in the simulation cell. The frequencies of rotational jumps for the four groups of molecules along the four possible axes of rotation, averaged over each group, are reproduced in Table 2. The numerical values of the frequencies span over 4 orders of magnitude, implying the existence of different dynamical modes in the crystal, as already suggested by the rotational self-correlation functions.

To rationalize the behavior of the functions $C_j(t)$ we developed a simple analytical model that derives these functions from the relative reorientation frequencies. We propose a master equation that describes the probabilities of occupation of the four available sites in the molecule for the Cl atoms. Let us define the stochastic variables Y_j that describe the position of the jth Cl atom on the four available sites. Then, each Y_j takes values over a range represented by {1,2,3,4}, with a probability distribution p_n^j over this range. Assuming that a reorientational jump in the molecule is a Markovian process, the master equation that describes the probability p_n^j of the state of Y_j is

$$\frac{dp_n^j(t)}{dt} = \sum_{n'} [\nu_{nn'}p_{n'}^j(t) - \nu_{n'n}p_n^j(t)];\ j = 1, \ldots, 4 \quad (2)$$

where $\nu_{nn'}$ is the transition probability per unit time from the site n' to the site n. These equations may be written in matrix form as

$$\frac{d\vec{P^j}}{dt} = V\vec{P^j} \quad (3)$$

where $\vec{P}$ is the vector $(p_1^j(t),p_2^j(t),p_3^j(t),p_4^j(t))$ and V is the 4×4 matrix

$$\begin{pmatrix} -(\nu_{21}+\nu_{31}+\nu_{41}) & \nu_{12} & \nu_{13} & \nu_{14} \\ \nu_{21} & -(\nu_{12}+\nu_{32}+\nu_{42}) & \nu_{23} & \nu_{24} \\ \nu_{31} & \nu_{32} & -(\nu_{13}+\nu_{23}+\nu_{43}) & \nu_{34} \\ \nu_{41} & \nu_{42} & \nu_{43} & -(\nu_{14}+\nu_{24}+\nu_{34}) \end{pmatrix} \quad (4)$$

Equation 3 is an homogeneous first-order differential equation with constant coefficients. The solution is

$$\vec{P^j}(t) = R^{-1}e^{V_D(t)}R\vec{P^j}(0) \quad (5)$$

Table 2. CCl_4 Average Reorientation Frequencies w_i (i = 1,...,4) (in ns^{-1}) for the Four Groups of Molecules about the Four Possible Directions of the Axis of Rotation[a]

	160 K				220 K			
axis	G_I	G_{II}	G_{III}	G_{IV}	G_I	G_{II}	G_{III}	G_{IV}
a_1	3.91×10^{-6}	7.81×10^{-7}	1.56×10^{-6}	7.81×10^{-7}	2.80×10^{-3}	1.62×10^{-4}	3.23×10^{-4}	1.51×10^{-3}
a_2	3.83×10^{-5}	2.11×10^{-5}	7.81×10^{-7}	3.43×10^{-5}	8.30×10^{-3}	5.39×10^{-3}	9.70×10^{-4}	1.20×10^{-2}
a_3	3.62×10^{-4}	1.00×10^{-2}	1.52×10^{-3}	7.42×10^{-5}	4.76×10^{-2}	4.26×10^{-1}	9.36×10^{-2}	1.78×10^{-2}
a_4	8.59×10^{-6}	6.02×10^{-5}	7.81×10^{-7}	2.34×10^{-6}	4.36×10^{-3}	1.76×10^{-2}	8.08×10^{-4}	2.53×10^{-3}

[a]For the fastest rotational axes the inverse of the frequency w_3 is a good approximation of the average waiting time between jumps (λ^{-1}).

DOI: 10.1021/acs.jpcb.5b11658
J. Phys. Chem. B XXXX, XXX, XXX−XXX

where R is the matrix that diagonalize V, $V_D = RVR^{-1}$. Assuming that C3 jumps are the exclusive mechanism of molecular reorientation, the $\nu_{nn'}$ can be approximated using the frequency of rotations w_i around the axes a_i. These frequencies were calculated from the MD simulations and are summarized in Table 2. They can be interpreted as the probabilities w_i for rotations per unit time around each one of the four possible axes. Frequencies smaller than 10^{-6} ns^{-1} correspond to fewer than five rotational jumps in 10 μs and therefore are negligible.

The tetrahedral constraint between the Cl atoms imply that a nn' transition can be achieved under two different single rotation events. Considering all rotation events as independent processes, we can calculate $\nu_{nn'}$ as the sum of the probability of the two possible events leading to a nn' transition. For example, $\nu_{12} = (w_3 + w_4)/2$, $\nu_{13} = (w_2 + w_4)/2$, $\nu_{14} = (w_2 + w_3)/2$, and so on. The factor of 1/2 is due to the assumption that both directions of rotation are equally probable, which was tested to be statistically true.

The next step is to solve the proposed master equation with the four different initial conditions, which are $P_1^j(0) = (1,0,0,0)$, $P_2^j(0) = (0,1,0,0)$, $P_3^j(0) = (0,0,1,0)$, and $P_4^j(0) = (0,0,0,1)$. Let us denote the four corresponding solutions as $p_i^j(t)$, with $i,j = 1,...,4$. Then, the rotational autocorrelation functions can be expressed in terms of the solution of the master equation as

$$C_j(t) = \vec{b}_j \cdot [\vec{b}_1 p_1^j(t) + \vec{b}_2 p_2^j(t) + \vec{b}_3 p_3^j(t) + \vec{b}_4 p_4^j(t)] \quad (6)$$

The resulting solutions $C_j(t)$ are plotted on Figure 2 using dashed lines. The agreement between the results directly measured from the simulation trajectories and those derived from the master equation is excellent, justifying the assumptions made in the derivation of the analytical model.

The statistics behind the rotational jumps can be evaluated by studying the waiting time between successive jumps around the axes $a_1,...,a_4$. On some of the axes the rotational events are very rare and the length of our simulations does not allow us to see a well-defined pattern for those specific slow axes. Nevertheless, for the fastest axes the process reveals itself as following a Poisson distribution. In Figure 3 we show the distribution of waiting times for rotational events around the fastest axis of rotation for each group of molecules. The histograms are directly obtained from the simulated trajectories. The solid red lines in the plots for the three fastest groups correspond to $e^{-\lambda t}$, with the Poisson parameter λ being the frequency of jumps around a_3 axes, w_3 from Table 2.

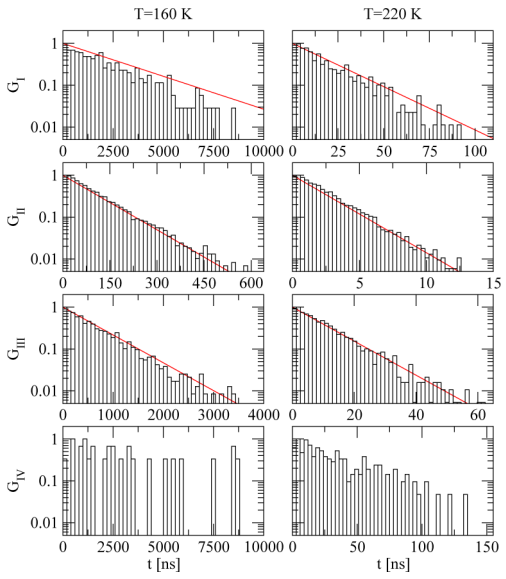

Figure 3. Distributions of waiting times for two temperatures and the corresponding Poisson curves (in red) for the fastest rotational axes of G_I, G_{II}, and G_{III}.

A similarity between the dynamical behavior of all of the different groups could be inferred by looking at the self-correlation functions $C_j(t)$ and distribution of waiting times shown in Figures 2 and 3, respectively. In particular, G_{II} and G_{III} are the two groups with the closest quantitative behavior. To explore whether this kinetic resemblance has a correlation with the molecular arrangement, we analyzed the orientation of the fastest axis for each one of the groups. Interestingly, the fastest axes of the molecules of G_{II} and G_{III} are parallel to each other in pairs that involve the first neighbors, as shown in Figure 4. For groups G_I and G_{IV} there is a certain degree of spacial correlation, but it does not include the eight pairs of molecules of the unit cell.

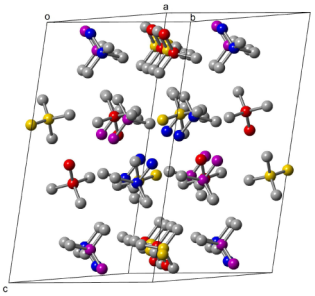

Figure 4. Unit cell displaying the molecules of groups G_I, G_{II}, G_{III}, and G_{IV} in red, blue, violet, and yellow, respectively. The colored axis represents the fastest direction of rotation for each molecule.

NQR spectroscopy allows us to measure the spin−lattice relaxation time T_1. Because the low-temperature crystalline structure of CCl_4 has four nonequivalent molecules in the unit cell, the NQR spectral lines correspond to the 16 Cl atoms of these four molecules. Then, it is possible to measure the relaxation times T_1, for each line, as a function of temperature. Because nuclear magnetization is proportional to the nuclear spin polarization, by applying the slow reorientational model for T_1 by Alexander and Tzalmona[35] it is possible to find the reorientation relaxation time as a function of the jumps probabilities ν_{nm}.

Starting from the master equation for the nuclear polarization, Zuriaga et al.[23] proposed a model for tetrahedral molecules that allow us to find the chlorine T_1 relaxation times as a function of reorientation frequencies w_i around the four molecular axes. From the analytical model and the MD simulations, 16 relaxation times are obtained at each temperature, 4 for each group of molecules. The results for T_1 versus $1000/T$ are represented in Figure 5 along with the experimental results, which also include the cases of $CBrCl_3$ and CBr_2Cl_2.

The existence of a preferential axis of rotation for three groups (G_I, G_{II} and G_{III}) allows the identification of three short times T_{1s} of similar magnitude (corresponding to the three Cl atoms out of the fastest axis) and a long time T_{1l} (for the Cl atom on the fastest axis). The remaining group (G_{IV}) has no preferential axis of rotation, and therefore the four relaxation times are all similar.

DOI: 10.1021/acs.jpcb.5b11658
J. Phys. Chem. B XXXX, XXX, XXX−XXX

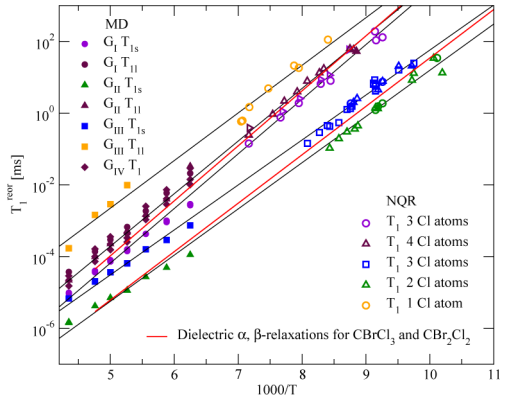

Figure 5. Spin−lattice relaxation times obtained by molecular dynamics simulations (full symbols). Results from NQR studies of CCl_4[23] (empty symbols) are shown. Red lines represents the behavior of τ_α (upper) and τ_β (lower) of $CBrCl_3$ and CBr_2Cl_2 taken from ref 23.

The set of 16 relaxation times from the simulations are grouped in increasing order in the following five sets:

1. The shortest time correspond to the T_{1s} describing G_{II} (green triangles).
2. The next time corresponds to T_{1s} of G_{III} (blue squares).
3. The third set is for T_{1s} of G_I (violet circles).
4. The fourth set includes T_{1l} of G_I (brown circles), T_{1l} of G_{II} (brown triangles), and T_1 of G_{IV} (brown diamonds).
5. The last set corresponds to T_{1l} of G_{III} (orange squares).

The black straight lines in Figure 5 are the result of a linear least-squares fit of the values log T_1 versus $1000/T$, including both, simulation and experimental results.

There are three main features that arise from Figure 5. First, the simulations curves are in a good agreement with the experimental data, prolonging the same Arrhenius curves from 100 to 230 K. Second, the results for T_1 spread along two orders of magnitude in time, indicating the presence of fast and slow modes. Third, the overall behavior resembles α and β relaxation times of CBr_2Cl_2 (also shown in Figure 5) and $CBrCl_3$, showing that the dynamics of the nonglass former CCl_4 has strong similarities with that of the other members of the isostructural series CBr_nCl_{4-n}.

CONCLUSIONS

We performed extensive molecular dynamics simulations of CCl_4 in the monoclinic cell. By studying time reorientational autocorrelation functions as a function of temperature we found distinct behaviors for the four different C−Cl bonds in the molecule. As a consequence, different reorientational correlations times emerge for the four groups of nonequivalent molecules in the system: Two times are enough to characterize three of the four groups and one time is associated with the remaining group.

The complete understanding of glassy systems, even in the case of the simpler rotational glasses, remains elusive in the sense that no complete theoretical picture can be drawn yet. Nevertheless, there is a general agreement on the existence of two main universal features referred to α and β relaxation. Rotational glasses of the type CBr_nCl_{4-n}, with n = 1, 2, 3, are glass formers displaying fast and slow rotational modes as they approach to the glass-transition temperature. We show that CCl_4 has essentially the same dynamical behavior, as a function of temperature, as that of its isostructural glass formers. Long molecular dynamics simulations trajectories, based on a simple pairwise additive force field, yield results that are fully in line with those obtained with NQR experiments. The simulations clearly show that there are preferential axes of rotation, which are fixed with respect to the crystal orientation. Two of the inequivalent group of molecules are significantly faster than the other two, leading to a clear heterogeneity in the dynamics of the system. Moreover, it is found that the orientation of the two fast axes of rotations is the same, suggesting an overall dynamics anisotropy correlated to the molecular orientations.

Finally, our results on CCl_4 suggest that the observed heterogeneous dynamic of molecules of type $CXCl_3$ with the same crystal structure could be due to the molecular environment on the crystal and not to the breaking of the tetrahedral symmetry of the molecule. Then, it would be interesting to corroborate if there is any relation between the fastest axis in the CCl_4 molecules and the C−Br axis in the $CBrCl_3$ crystals. We are performing MD simulations to elucidate this open question.

ASSOCIATED CONTENT

Supporting Information

The Supporting Information is available free of charge on the ACS Publications website at DOI: 10.1021/acs.jpcb.5b11658.

More detailed explanation of the method for counting molecular jumps and C−C radial distribution functions at the lowest and highest simulated temperatures along with experimental C−C distances. (PDF)

AUTHOR INFORMATION

Corresponding Authors

*N.B.C.: Phone: +54(0)3514334051, ext. 218. Fax: +54(0) 3514334054. E-mail: ncaballe@famaf.unc.edu.ar.
*M.Z.: E-mail: zuriaga@famaf.unc.edu.ar.
*M.C.: E-mail: mcarignano@qf.org.qa.
*P.S.: E-mail: serra@famaf.unc.edu.ar.

Notes

The authors declare no competing financial interest.

ACKNOWLEDGMENTS

N.B.C., M.Z., and P.S. acknowledge financial support of SECYTUNC and CONICET. This work used computational resources from CCAD Universidad Nacional de Córdoba (http://ccad.unc.edu.ar/), in particular the Mendieta Cluster, which is part of SNCAD MinCyT, República Argentina.

REFERENCES

(1) Schneider, U.; Brand, R.; Lunkenheimer, P.; Loidl, A. Excess Wing in the Dielectric Loss of Glass Formers: A Johari-Goldstein β-Relaxation? *Phys. Rev. Lett.* **2000**, *84*, 5560−5563.
(2) Lunkenheimer, P.; Loidl, A. Dielectric Spectroscopy of Glass-forming Materials: α-relaxation and Excess Wing. *Chem. Phys.* **2002**, *284*, 205−219.
(3) Affouard, F.; Cochin, E.; Danéde, F.; Decressain, R.; Descamps, M.; Haeussler, W. Onset of Slow Dynamics in Difluorotetrachloroethane Glassy Crystal. *J. Chem. Phys.* **2005**, *123*, 084501.
(4) Ngai, K. L.; Paluch, M. Classification of Secondary Relaxation in Glass-Formers Based on Dynamic Properties. *J. Chem. Phys.* **2004**, *120*, 857−873.
(5) Pardo, L. C.; Lunkenheimer, P.; Loidl, A. α and β Relaxation Dynamics of a Fragile Plastic Crystal. *J. Chem. Phys.* **2006**, *124*, 124911.

(6) Johari, G. P.; Goldstein, M. Viscous Liquids and the Glass Transition. II. Secondary Relaxations in Glasses of Rigid Molecules. *J. Chem. Phys.* **1970**, *53*, 2372.
(7) Ngai, K. L. Correlation Between the Secondary β-relaxation Time at T_g with the Kohlrausch Exponent of the Primary α Relaxation or the Fragility of Glass-Forming Materials. *Phys. Rev. E: Stat. Phys., Plasmas, Fluids, Relat. Interdiscip. Top.* **1998**, *57*, 7346−7349.
(8) Schneider, U.; Brand, R.; Lunkenheimer, P.; Loidl, A. Excess Wing in the Dielectric Loss of Glass Formers: A Johari-Goldstein β Relaxation? *Phys. Rev. Lett.* **2000**, *84*, 5560−5563.
(9) Johari, G. P.; Power, G.; Vij, J. K. Localized Relaxationś Strength and its Mimicry of Glass-softening Thermodynamics. *J. Chem. Phys.* **2002**, *116*, 5908−5909.
(10) Johari, G. P. Intrinsic Mobility of Molecular Glasses. *J. Chem. Phys.* **1973**, *58*, 1766−1770.
(11) Capaccioli, S.; Ngai, K. L.; Shinyashiki, N. The Johari-Goldstein β-Relaxation of Water. *J. Phys. Chem. B* **2007**, *111*, 8197−8209.
(12) Capaccioli, S.; Ngai, K. L. Resolving the Controversy on the Glass Transition Temperature of Water? *J. Chem. Phys.* **2011**, *135*, 104504.
(13) Jiménez-Ruiz, M.; Criado, A.; Bermejo, F. J.; Cuello, G. J.; Trouw, F. R.; Fernández-Perea, R.; Löwen, H.; Cabrillo, C.; Fischer, H. E. Purely Dynamical Signature of the Orientational Glass Transition. *Phys. Rev. Lett.* **1999**, *83*, 2757−2760.
(14) Jiménez-Ruiz, M.; González, M. A.; Bermejo, F. J.; Miller, M. A.; Birge, N. O.; Cendoya, I.; Alegría, A. Relaxational Dynamics in the Glassy, Supercooled Liquid, and Orientationally Disordered Crystal Phases of a Polymorphic Molecular Material. *Phys. Rev. B: Condens. Matter Mater. Phys.* **1999**, *59*, 9155−9166.
(15) Vogel, M.; Rossler, E. On the Nature of Slow β-Process in Simple Glass Formers: A ^{2}H NMR Study. *J. Phys. Chem. B* **2000**, *104*, 4285−4287.
(16) Vogel, M.; Rossler, E. Slow β Process in Simple Organic Glass Formers Studied by one- and two-dimensional 2H Nuclear Magnetic Resonance. I. *J. Chem. Phys.* **2001**, *114*, 5802.
(17) Romanini, M.; Negrier, Ph.; Tamarit, J. Ll.; Capaccioli, S.; Barrio, M.; Pardo, L. C.; Mondieig, D. Emergence of Glassy-like Dynamics in an Orientationally Ordered Phase. *Phys. Rev. B: Condens. Matter Mater. Phys.* **2012**, *85*, 134201.
(18) Drozd-Rzoska, A.; Rzoska, S. J.; Pawlus, S.; Tamarit, J. L. Dynamics Crossover and Dynamic Scaling Description in Vitrification of Orientationally Disordered Crystal. *Phys. Rev. B: Condens. Matter Mater. Phys.* **2006**, *73*, 224205.
(19) Martinez-Garcia, J. C.; Tamarit, J. L.; Rzoska, S. J. Prevalence for the Universal Distribution of Relaxation Times Near the Glass Transitions in Experimental Model systems: Rodlike Liquid Crystals and Orientationally Disordered Crystals. *J. Chem. Phys.* **2011**, *134*, 144505.
(20) Martinez-Garcia, J. C.; Tamarit, J. L.; Rzoska, S. J. Enthalpy Space Analysis of the Evolution of the Primary Relaxation Time in Ultraslowing Systems. *J. Chem. Phys.* **2011**, *134*, 024512.
(21) Martinez-Garcia, J. C.; Tamarit, J. L.; Capaccioli, S.; Barrio, M.; Veglio, N.; Pardo, L. C. α-relaxation Dynamics of Orientanionally Disordered Mixed Crystals Composed of Cl-adamantane and CN-adamantane. *J. Chem. Phys.* **2010**, *132*, 164516.
(22) Caballero, N. B.; Zuriaga, M.; Carignano, M.; Serra, P. The Plastic and Liquid Phases of CCl_3Br Studied by Molecular Dynamics Simulations. *J. Chem. Phys.* **2012**, *136*, 094515.
(23) Zuriaga, M. J.; Perez, S. C.; Pardo, L. C.; Tamarit, J. Ll. Dynamic Heterogeneity in the Glass-Like Monoclinic Phases of CBr_nCl_{4-n}, n = 0,1,2. *J. Chem. Phys.* **2012**, *137*, 054506.
(24) Zuriaga, M.; Pardo, L. C.; Lunkenheimer, P.; Tamarit, J. Ll.; Veglio, N.; Barrio, M.; Bermejo, F. J.; Loidl, A. New Microscopic Mechanism for Secondary Relaxation in Glasses. *Phys. Rev. Lett.* **2009**, *103*, 075701.
(25) Pardo, L. C.; Barrio, M.; Tamarit, J. L.; López, D. O.; Salud, J.; Negrier, P.; Mondieig, D. Miscibility Study in Stable and Metastable Orientational Disordered Phases in a Two-Component System $(CH_3)CCl_3$+CCl_4. *Chem. Phys. Lett.* **1999**, *308*, 204−210.
(26) Pardo, L. C.; Barrio, M.; Tamarit, J. L.; López, D. O.; Salud, J.; Negrier, P.; Mondieig, D. First Experimental Demonstration of Crossed Isodimorphism: $(CH_3)_3CCl$ + CCl_4 Melting Phase Diagram. *Phys. Chem. Chem. Phys.* **2001**, *3*, 2644−2649.
(27) Pardo, L. C.; Barrio, M.; Tamarit, J. L.; Negrier, P.; López, D. O.; Salud, J.; Mondieig, D. Stable and Metastable Phase Diagram of the Two-Component System $(CH_3)_3CCl$-$(CH_3)CCl_3$: An Example of Crossed Isodimorphism. *J. Phys. Chem. B* **2001**, *105*, 10326−10334.
(28) Pardo, L. C.; Barrio, M.; Tamarit, J. L.; López, D. O.; Salud, J.; Negrier, P.; Mondieig, D. Stable and Metastable Orientationally Disordered Mixed Crystals of the Two-Component System $(CH_3)_2CCl_2$+CCl_4. *Chem. Phys. Lett.* **2000**, *321*, 438−444.
(29) Pothoczki, Sz.; Ottochian, A.; Rovira-Esteva, M.; Pardo, L. C.; Tamarit, J. Ll.; Cuello, G. J. Role of Steric and Electrostatic Effects in the Short-Range Order of Quasitetrahedral Molecular Liquids. *Phys. Rev. B: Condens. Matter Mater. Phys.* **2012**, *85*, 014202.
(30) Ohta, T.; Yamamuro, O.; Matsuo, T. Heat Capacities and Phase Transitions of $CBrCl_3$ and CBr_2Cl_2. *J. Phys. Chem.* **1995**, *99*, 2403−2407.
(31) Binbrek, O. S.; Lee-Dadswell, S. E.; Torrie, B. H.; Powell, B. M. Crystal Structures of Dibromodichloromethane and Bromotrichloromethane. *Mol. Phys.* **1999**, *96*, 785−794.
(32) Zuriaga, M.; Carignano, M.; Serra, P. Rotational Relaxation Characteristics of the Monoclinic Phase of CCl_4. *J. Chem. Phys.* **2011**, *135*, 044504.
(33) Cohen, S.; Powers, R.; Rudman, R. Polymorphism of the Crystalline Methylchloromethane Compounds. VI. The Crystal and Molecular Structure of Ordered Carbon Tetrachloride. *Acta Crystallogr., Sect. B: Struct. Crystallogr. Cryst. Chem.* **1979**, *35*, 1670−1674.
(34) Carter, N. J.; Cross, A. Mechanics of the Kinesin Step. *Nature* **2005**, *435*, 308.
(35) Alexander, S.; Tzalmona, A. Measurement of Molecular Rotation by N^{14} Nuclear Quadrupole Resonance Relaxation Times. *Phys. Rev. Lett.* **1964**, *13*, 546−547.

DOI: 10.1021/acs.jpcb.5b11658
J. Phys. Chem. B XXXX, XXX, XXX−XXX